Theoretical surface-enhanced Raman spectra study of substituted benzenes I. Density functional theoretical SERS modelling of benzene and benzonitrile

Guillermo Diaz Fleming [a,*], Italo Golsio [a], Andres Aracena [a], Freddy Celis [a], Leticia Vera [a], Rainer Koch [b], Marcelo Campos-Vallette [c]

[a] *Department of Chemistry, Faculty of Sciences, University of Playa Ancha, Valparaiso, Casilla 34-V, Chile*
[b] *Institute for Pure and Applied Chemistry and Center of Interface Science, University of Oldenburg, P.O. Box 2503, D-26111 Oldenburg, Germany*
[c] *Molecular Spectroscopy Laboratory, Department of Chemistry, Faculty of Sciences, University of Chile, Casilla 653, Santiago, Chile*

A B S T R A C T

This paper reports a DFT modelling of SERS spectra for benzene and benzonitrile on the basis of a simple noncoordinate substrate–adsorbate model. Assignment of normal modes was obtained from internal force constants and potential energy distribution matrices and used to identify, according the SERS selection rules, the orientation of the optimized molecules on the metallic surface. Calculated band enhancements are in good agreement with experimental observations. The optimized geometry parameters of the molecule–Ag system, changes of HOMO–LUMO energies are discussed to give insight in the different SERS mechanisms for both molecules.

Keywords:
DFT calculations
SERS spectra modelling
Benzene
Benzonitrile

1. Introduction

It is well known that adequate prediction and interpretation of the vibrational spectra requires the use of quantum chemical methods [1]. In this sense, different ab initio studies on IR and Raman have been performed since a decade, and more recently these studies have been extended to surface-enhanced Raman scattering (SERS) [2]. With the recent progress in developing useful approximate functionals and availability of versatile software, density functional theory (DFT) has become a popular approach for the computation of molecular structure, vibrational frequencies and energies of chemical reactions [3–5], because vibrational calculations are computational less demanding than the conventional ab initio correlation techniques such as the second order Möller-Plesset (MP2) method [6]. DFT has been reported to provide excellent vibrational frequencies of organic compounds if the calculated frequencies are scaled to compensate for the approximate treatment of electron correlation, for basis set deficiencies, and for the anharmonicity [7].

The benzonitrile (BN) molecule and some of its derivatives have been widely studied because of their interesting biochemical and physical properties [8–13].From a theoretical point of view, BN is interesting because it contains different binding sites for its interaction with the metal surface. Thus, BN contains an aromatic ring, the π bond of the CN group, and lone pair electrons of nitrogen atom [14]. In this sense, Raman and SERS spectroscopic studies of BN [15] and its methoxy derivatives [16] in silver sol have been reported while the orientation of adsorbed benzene and BN on gold–aqueous interface and on gold in vacuum at 20 K have been analyzed by Gao et al. [17] Further, SERS for BN adsorbed on seven electrode surfaces was studied by Weaver and coworkers [18] in combination with DFT calculations to give insight into the underlying structural reasons for the sensitivity of the experimental coordination-induced frequency shifts to the nature of the intramolecular mode and the metal surface. Palafox et al. [19] have performed a theoretical study of vibrational frequencies for difluorbenzonitriles at different semiemprical, SCF, post-SCF and DFT levels of theory.

Taking into account that Refs. [15–17] provide only qualitative evidence that SERS selection rules can yield reliable information regarding adsorbate orientation on metal surface, and that in Ref. [18] the DFT calculation was performed on a structure with Ag coordination to the terminal nitrogen atom, we report here a more comprehensive theoretical DFT modelling of SERS spectra for BN on the basis of a simple noncoordinate substrate–adsorbate model with a twofold purpose: first, to complete the information about the possible site of the adsorbate–substrate interaction, and second, to derive the orientation of the molecules on the surface and to gain insight on the spectral assignment. This work also deals with the mechanisms proposed to explain the main contributions to the overall SERS phenomenon-charge transfer and electromagnetic

* Corresponding author. Tel.: +56 32 500276; fax: +56 32 7688.
E-mail address: ruben_diaz@entelchile.net (G.D. Fleming).

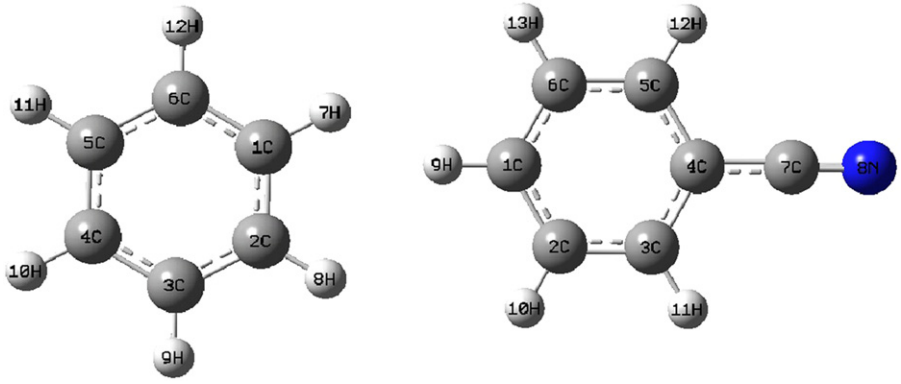

Fig. 1. B3LYP/LANL2DZ-optimized benzene and BN geometries.

[20] in order to identify the one which could be dominant in our metal–molecule system, and, consistently, to interpret the interaction as a physisorption or a chemisorption.

This study also requires the Raman and SERS modelling of benzene in order to compare the interaction of the metallic surface with the aromatic ring and changes by the effect of the CN group. It provides information on the force constants for all molecules under study to test the validity of the calculation.

2. Computational details

Calculations of the structure and vibrational spectra of the investigated compounds were performed using the Gaussian 03 program package [21]. All calculations were carried out with Becke's three-parameter hybrid method using the Lee–Yang–Parr correlation functional (B3LYP) [22,23] together with the LANL2DZ basis set corresponding to the D95 basis on first row atoms [24] and the Los Alamos DZ on silver [25]. For the optimized structure of the examined species no imaginary frequencies modes were obtained, proving that a local minimum on the potential energy surface was found. The energies of the frontier orbitals discussed in the last section are in fact those of the β orbitals, close examination showed that there is almost no difference to the corresponding α orbitals which the additional α spin orbital (a HOMO) being located purely on the Ag atom.

Calculated wave numbers have been scaled by 0.9695 to account for anharmonic behavior. This value has been applied to all regions of the spectra, so it is possible that some vibrations are affected stronger than others [26].

Force constants obtained in Cartesian coordinates with Gaussian were transformed into internal force constants through FCART 01, which is a modification of a previous software [27] written to accomplish all the necessary transformation and calculations using the G03 output. With the internal force constants matrices of the potential energy distribution (PED) are obtained which provide a measure of each internal coordinate's contribution to the normal coordinate at the above-mentioned theoretical level. For the sake of brevity, the complete tables of the internal force constants and PED are not reported here, but can be downloaded as supporting material.

The surface was modelled by a single Ag atom, at an initial distance of 3.0 Å in a position near perpendicular to a C atom and to the CN group for benzene and BN, respectively. No constraints were used for the calculation during the geometry optimization of the adsorbate–surface system. While a single atom model to represent a metallic surface is not quantitative, this arrangement mimics adequately the coordinative effects upon the aromatic intramolecular bonding of interest here [18,28,29]. Also, this approach has the advantage of computational efficiency so that the individual calculated harmonic vibrational modes can readily be compared to those of the normal Raman spectra.

The methodology to investigate the electronic properties of our molecules on the silver substrate basically consists of five steps:

(1) Geometry optimization of free molecules.
(2) Determination of the equilibrium position of the molecule and the Ag atom.
(3) Comparison of calculated Raman and SERS frequencies and intensities.
(4) Analysis of the angle variation between molecules and the silver atom as a consequence of the geometry optimization.
(5) Analysis of the molecular orbitals and the corresponding energies for the free molecules and the molecules interacting with silver atom.

Table 1
Comparison of calculated and experimental bond lengths (Å) of benzene and BN

	Benzene	BN					
	(a) Calc.	(a) Calc.	(b) MW	(c) ED	(d) NMR	(e) HF/4-21G	(f) HF/6-31G**
R(2,3)	1.409	1.416	1.396		1.408	1.400	1.390
R(1,2)	1.409	1.405	1.391	1.400	1.398	1.391	1.383
R(5,6)	1.409	1.409	1.399		1.400	1.395	1.386
R(3,12)		1.440	1.444	1.438	1.434	1.437	1.445
R(12,13)		1.183	1.156	1.168	1.166	1.156	1.137
R(1,7)	1.088	1.086	1.088		1.073	1.076	1.074
R(2,8)	1.088	1.087	1.087	1.086	1.089	1.076	1.075
R(5,11)	1.088	1.087	1.084		1.083	1.077	1.076

(a) Present work; (b) Ref. [30]: average microwave structure; (c) Ref. [31]: electron diffraction structure; (d) Ref. [32]: liquid–crystal NMR structure; (e) Ref. [33]; (f) Ref. [34].

Table 2
Stretching (mdyn/Å) and bending (mdyn, Å/rad^2) force constants for benzene and BN

	Benzene		BN	
	(a)	(b)	(a)	(c)
f_{CC}	5.294	6.493	5.270[a]	6.470
f_{CH}	5.631	5.066	5.690	5.190
f_{C-CN}			5.799	5.400
f_{CN}			17.560	17.574
f_{CCC}	0.716	0.754	0.705	0.740
f_{CCH}	0.449	0.515	0.449	0.520
f_{CCN}			0.365	0.300

[a] Average. (a) This work; (b) Ref. [36]; (c) Ref. [33].

3. Results and discussion

3.1. Raman spectrum modelling of benzene and benzonitrile

Fig. 1 shows the optimized benzene and BN molecules. The calculated geometrical parameters of these molecules represent quite well the sp^2 hybridization of the ring system. In Table 1 are presented calculated and experimental bond length parameters. For BN, the CC bonds show some variation as a consequence of the CN group, in comparison with benzene. This group shows a bond length of 1.18 Å which is characteristic for a triple bond, modified by electron contribution from the C(3)–C(12) bond, contributing to the conjugation of the system. These results are in good agreement with the experimental data obtained by microwave spectroscopy [30], electron diffraction [31], NMR [32], and with those obtained in other theoretical studies [33,34].

In Table 2 are collected a selection of stretching and bending diagonal force constants for benzene and BN obtained at our level of calculation. These calculated values are in good agreement with those expected for aromatic systems, although the DFT method underestimates C–C stretching values and overestimates C–CN and CN values due partly to the neglect of electron correlation and partly to basis set truncation. Interaction force constants between internal coordinates without atoms in common have similar values than those thoroughly discussed Neto et al. [35] and are hence not given here. Values presented for benzene are comparable to those given in an empirical work performed by La Lau and Snyder [36], as well as in a HF calculation by Pulay et al. [37], while the BN data are comparable to those calculated in Ref. [33].

Table 3
Selected calculated and experimental Raman wavelengths (cm^{-1}), intensities (Å^4/amu) and band assignment for benzene

Symmetry	Exp.[a]	Calc.	Raman Int.	Assignment
A_{1g}	992	974	67	Ring breathing
	3063	3097	104	CH stretching symm
A_{2u}	(671)	687	0	CH bending out-of-plane asymm
B_{2u}	(1150)	1165	0	CH in-plane bending
	(1308)	1333	0	Ring deformation in-plane asymm
E_{1g}	847	861	0	CH bending out-of-plane
E_{1u}	(1038)	1018	0	CH bending in-plane asymm
	(1478)	1459	0	CH bending in-plane asymm
E_{2g}	604	604	7	Ring deformation in-plane symm
	1176	1176	7	CH bending in-plane symm
	1585	1591	14	CC stretching symm
	3044	3087	0	CC stretching asymm
E_{2u}	(404)	404	0	Ring deformation out-of-plane
	(975)	989	0	CH bending out-of-plane

[a] Ref. [17], frequencies in parenthesis are Raman inactive.

Table 4
Selected calculated and experimental Raman wavelengths (cm^{-1}), intensities (Å^4/amu) and band assignment for BN

Symmetry	Exp. (a)	(b)	Calc.	Raman Int.	Assignment
A_1	462	461	452	8	CCC bending in-plane
	768	770	783	0	CH bending out-of-plane asymm
	1002	1001	983	45	CCC trigonal breathing
	1027	1026	1018	8	CH bending in-plane
	1180	1176	1184	27	CH bending in-plane
	1194	1192	1188	13	C–CN stretching
	1490	1492	1474	2	CC stretching in-plane CH bending in-plane
	1599	1598	1573	4	CC stretching in-plane CH bending in-plane
	3065		3124	50	CH stretching symm
A_2	400[c]	401	402	0	CCC bending out-of-plane asymm
	848[c]				
B_1	383		382	3	Ring-C–N bending out-of-plane
	551	547	547	4	CCC bending out-of-plane, ring-CN bending out-of-plane
	690		699	0	CH bending out-of-plane
	754	755	746	12	CH bending out-of-plane symm
	926	925	949	0	CH bending out-of-plane
B_2	626	626	620	5	CCC bending in-plane
	1162		1173	5	CH bending in-plane
	1290[c]	1289	1313	0	CH bending in-plane
	1336[c]	1337	1337	3	CC stretching in-plane
	1449	1448	1430	2	CC stretching in-plane CH bending in-plane
	1584	1603	1600	92	CH bending in-plane symm, ring deformation in-plane
A_1	2232	2230	2195	401	CN stretching

(a) Ref. [18]; (b) Ref. [17]; (c) Ref. [38].

In Tables 3 and 4 are presented selected frequencies, Raman intensities and current assignment for benzene and BN, respectively, as well as experimental values given in the literature. The assignment agrees well with our PED matrix calculation, and the calculated band intensities are in good agreement with the experimental data. The most intense bands currently observed in the benzene Raman spectrum at about 1000 and 3000 cm^{-1} are calculated with high intensity at 974 and 3097 cm^{-1}. Weak bands reported at 1585 and 1176 cm^{-1} are calculated also with a lower intensity at 1591 and 1176 cm^{-1}. Very weak bands at 604 and 847 cm^{-1}, are reproduced at 604 and 861 cm^{-1}. For BN, more intense experimental Raman bands at 2230, 3065, 1603, 1192, 1176 and 1001 cm^{-1}, are calculated to 2230, 3124, 1600, 1188, 1184 and 983 cm^{-1}, with the same intensity pattern.

3.2. SERS spectrum modelling of benzene and BN

The hypothesis of this work is that the variation of the angle between the molecule and the Ag atom from the initial to the calculated equilibrium position should be proportional to the SERS effect, and consequently produce intensity and/or frequency variation of some specific bands. Figs. 2 and 3 show the change of the silver atom position during the optimization for benzene and BN, giving quite opposite effect in both systems. In the case of benzene, the Ag atom appear closer to the centre of the aromatic ring (flat orientation) at an average C–Ag distance of 3.8 Å, while in the case of BN the Ag atom becomes more in line to the nitrogen atom at a distance of 2.57 Å, with a C–N–Ag angle of 154° (tilted orientation). Table 5 yields selected bond distances.

In Table 6, we present force constants for benzene and BN obtained with data of the SERS spectra. Slight differences with those

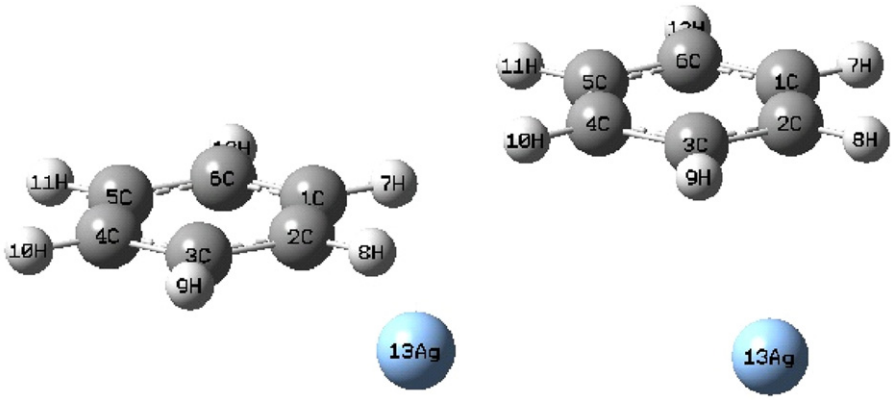

Fig. 2. Benzene–Ag orientation before (left) and after the optimization (right).

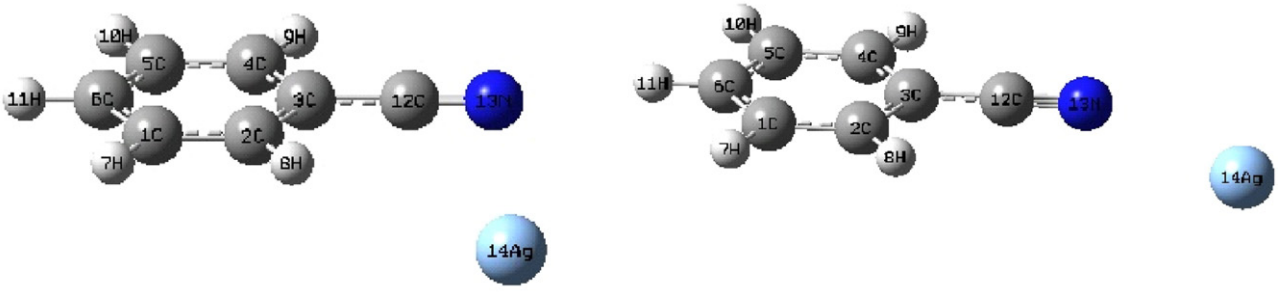

Fig. 3. BN–Ag orientation before (left) and after the optimization (right).

Table 5
Selected optimized bond lengths (Å) of the benzene–Ag and BN–Ag systems

	Benzene–Ag	BN–Ag
R(1,2)	1.411	1.404
R(1,6)	1.410	1.410
R(1,7)	1.088	1.087
R(1,Ag)	3.569	
R(2,3)	1.410	1.417
R(2,8)	1.088	1.086
R(2,Ag)	3.571	
R(3,4)	1.409	1.417
R(4,5)	1.409	1.404
R(5,6)	1.409	1.410
R(7,Ag)	3.885	
R(8,Ag)	3.889	
R(12,Ag)		3.663
R(N13,Ag)		2.566
R(12-N13)		1.180

Table 6
SERS stretching (mdyn, Å), bending (mdyn, Å/rad^2) and torsion (mdyn, Å/rad^2) force constants for benzene–Ag and BN–Ag complexes

	Benzene–Ag	BN–Ag
f_{CC}	5.25	5.39
f_{CH}	5.63	5.69
f_{C-CN}		5.80
f_{CN}		17.50
f_{NAG}		0.16
f_{CCC}	0.71	0.71
f_{CCH}	0.45	0.45
f_{CNAg}		0.16
f_{CCN}		0.46
f_{CCCC}	0.042	0.042
f_{CCH}	0.039	0.039
f_{HCCH}	0.041	0.040

obtained from the Raman spectra reflect the presence of the Ag atom. In the case of BN–Ag, force constants involving the Ag atom are in the expected range. The lower force constant value of CN after the SERS effect is consistent with a N–Ag binding, which debilitates the CN bond.

3.3. Mechanism analysis

The two most important mechanisms that contribute to the overall enhancement are related to an increase in both the molecular polarization α of the absorbed species and the local electric field (E_{local}) near the metallic surface [20,39–41]. The former account for the chemical or charge transfer (CT) mechanism, which depends sensitively on the details of the chemical bonding between adsorbate and substrate. It is a kind of resonance Raman scattering in which the resonant intermediate states are thought to arise from metal–molecules charge transfer excitation, that is, if the difference in energy between the Fermi level (which give us information of the electrons that take part in ordinary electrical conductivity) and the frontier orbital (HOMO–LUMO) of the absorbed species is close in frequency to the incident light, an enhancement mechanism occurs [42]. The interaction between the metal and molecule will be maximized when the HOMO–LUMO separation is resonant with the excitation wavelength [43]. If the LUMO is too high in energy with respect to the Fermi level, or the HOMO similarly lies too low in energy, neither the excited electrons nor holes in the metal can efficiently couple to the molecule. The CT process would enhance the symmetrical modes in general, and preferentially modes involving coordinates which are relaxed by the electronic exited state [44].

In the second case, the electromagnetic fields of the exciting laser and Raman scattering are amplified by the excitation of surface plasmons on structures with nanoscale roughness (or particle sizes) on the order of 100 nm. This EM mechanism, which is oper-

Table 7
Comparison between Raman and SERS frequencies (cm^{-1}) and intensities ($Å^4$/amu) for benzene

Symm.	Exp. freq.[a]		Calc. freq.		Calc. intensities			Assignment
	SERS	Raman	SERS	Raman	SERS	Raman	Ratio[c]	
A_{1g}	982	992	972	974	65	67	1.0	Ring breathing
	3060	3063	3088	3097	0.2	104	0.0	CH stretching in-plane symm
A_{2u}	697	671[b]	693	687	2	0	–	CH bending out-of-plane symm
B_{2u}	(1149)	1150[b]	1165	1165	0	0	–	CH bending in-plane symm
	1311	1308[b]	1331	1333	0	0	–	CC stretching in-plane asymm
E_{1g}	864	847	865	861	3	0	–	CH bending out-of-plane asymm
E_{1u}	(1032)	1038[b]	1021	1018	0	0	–	CH bending out-of-plane
	1473	1478[b]	1458	1459	0.4	0	–	CC stretching in-plane
E_{2g}	(605)	604	604	604	5	7	0.7	Ring deformation in-plane asymm
	1174	1176	1175	1176	6	7	0.9	CH bending in-plane
	1587	1585	1588	1591	10	14	0.7	CC stretching symm
E_{2u}	397	404[b]	400	404	1	0	–	Ring deformation out-of-plane asymm

[a] Ref. [17], frequencies in parenthesis are very weak.
[b] Frequencies inactive in Raman.
[c] "–" Raman intensity is zero, ratio not defined.

ative for in certain metals, can account for enhancement factors of 10^4 to 10^6, whereas the chemical contribution is thought to be of the order 10^2. Most authors now agree that both mechanisms contribute to the overall effect (multiplicatively), however one or other can be dominant for certain systems.

While calculations performed on models based on the EM mechanism predict that intensities enhancement are produced at significant distances of the surface [45], the CT mechanism is limited to those molecules adsorbed on the metal (chemi- or physisorbed).

SERS selection rules which can be inferred from both CT and EM mechanisms [46] consider that vibrations with polarizability tensor normal to the surface suffer the highest intensity enhancement, because the vibration implies electronic displacements which interact with the electromagnetic field produced by the surface plasmons (electron oscillations at the metallic surface). In such a case, assignment of those bands which increase its intensity give insight on the orientation of the molecule on the surface. The SERS effect is stronger in molecules with electron lone pairs and also in molecules with π electron density. According to Figs. 2 and 3 and

Table 8
Comparison between Raman and SERS frequencies (cm^{-1}) and intensities ($Å^4$/amu) for BN

Symm.	Exp. freq.[a]		Calc. freq.		Calc. intensities			Assignment
	SERS	Raman	SERS	Raman	SERS	Raman	Ratio[c]	
A_1	480	462	458	452	656	8	82.0	CCC bending in-plane
	775	768	748	746	180	12	15.0	Ring breathing
	999	1002	983	983	691	45	15.4	CCC trigonal breathing
	1025	1027	1018	1018	3	8	0.4	CH bending in-plane
			1174	1173	11	5	2.2	CH bending in-plane
	1177	1180	1184	1184	1739	27	64.4	CH bending in-plane
	1197	1194	1190	1188	28	13	2.2	CH bending in-plane
	1488	1490	1473	1474	274	2	137.0	CC stretching in-plane
	1595	1599	1596	1600	6249	92	67.9	CC stretching in-plane
A_2	385	(400)	384	402	96	0	–	CC bending out-of-plane
	862	(848)		863	0	0	–	CH bending out-of-plane asymm
B_1	550	551	557	547	17	4	4.3	CCC bending out-of-plane
	758	754	776	746	8	12	0.7	CH bending out-of-plane
	930	(926)	944	949	2	0	–	CH bending out-of-plane
B_2	626	626	621	620	6	5	1.2	CCC bending in-plane
		1162						
		(1290)						
	1390	(1336)	1338	1337	18	3	6.0	CC stretching in-plane asymm
	1448[b]	1449	1430	1430	10	2	5.0	CC stretching in-plane symm
Ag effect on BN internal coordinates								
	2242	2230	2183	2195	27357	401	68.2	CN stretching
			179		3			Deformation Ring-CCN
			164		14			Deformation BN
			81		256			Deformation Ag–BN
			44		1			Stretching Ag–BN
			39		101			Deformation Ag–BN

[a] Ref. [18], frequencies in parenthesis extracted from Ref. [38].
[b] Ref. [15].
[c] "–" Raman intensity is zero, ratio not defined.

Tables 7 and 8 for benzene SERS the aromatic π system is important, while for BN it is the lone pair of the CN group.

3.4. Analysis of band shifts

It is also observed in Tables 7 and 8 that shifting of Raman–SERS frequencies for both molecules in the modelled spectra follows, in general, the same trend as the experimental ones. It is useful to examine the shift of the breathing frequencies of these molecules, in which a red shift of about 10 cm^{-1} occurs as a consequence of the bond weakening in the benzene ring system caused by the back donation of the metal *d*-electrons to the benzene ring π^* antibonding orbitals. In our calculations of the benzene Raman spectrum, the band at 974 cm^{-1} is shifted to 972 cm^{-1} in the SERS spectrum of this molecule. This small shifting indicates a weak interaction benzene–Ag. For the benzonitrile molecule, there are two kind of ring breathing modes namely ν_1 and ν_{12}: [35] the ν_1 (746 cm^{-1}) ring mode is slightly blue shifted in the SERS spectrum to 748 cm^{-1}, whereas the ν_{12} (983 cm^{-1}) trigonal ring breathing mode obtained in the modelled Raman spectrum remains in the same position in the modelled SERS spectrum. This is in agreement with the experimental observation [35] in the sense that mono-substituted benzene ν_1 is more sensitive to the mass of the substituent than other ring modes, so that the blue shifting is a consequence of the substituent mass effect rather than the interaction between the benzene ring π orbital and the metal d orbital. These results support quite well our simple model. In general, calculated Raman frequencies shifting as a consequence of the molecule–Ag interaction are in good agreement with experimental ones, with exception of the CN mode where the shift is in the opposite direction. This could be due to the sensitivity of the Ag–N interaction where small geometrical changes lead to changes of the calculated SERS for ν_{CN} of up to 30 cm^{-1} [47]. The similarity of the calculated ν_{CN} SERS and Raman values are the consequence of the participation of both π and lone pair electrons of the CN group interacting with the Ag surface. This result correlates well with observed SERS and Raman CN frequencies [15] which also do not differ much.

3.5. Orientation analysis

The molecular orientations observed in Figs. 2 and 3 are confirmed by the comparison of intensity in Raman and SERS spectra on the basis of the corresponding assignment (Tables 7 and 8). Enhanced bands should be those belonging to vibrations normal to the surface.

For benzene, bands enhancements are in agreement with observed intensity difference between Raman and SERS spectra [17]. Enhanced Raman bands are those at about 671 (CH bending out-of-plane symm), 847 (CH bending out-of-plane asymm) and at 404 cm^{-1} (out-of-plane ring deformation). These bands possess strong polarizability tensors perpendicular to the metallic surface. The intense bands at 992 (ring breathing) and the weak one at 604 cm^{-1} (in-plane ring deformation) retain the same intensity. The small increase in intensity of the inactive Raman band at 1478 cm^{-1} can be due to the influence of the CH in-plane bending, because the small inclination of benzene on the Ag surface and infer to π bonding interaction of the benzene molecule with the Ag atom.

With respect to the quasilinearity of the optimized BN–Ag system, its distinct normal modes can be classified in the irreducible representation of the C_{2v} point group. Table 8 shows that the most strongly enhanced bands belong to in-plane vibrations, with the biggest enhancement the one corresponding to CN stretching. It is furthermore possible to compare the calculated SERS intensities with the experimental values of electrochemistry Au adsorbed BN [18], where calculated enhanced intensities clearly coincide with the increasing in intensity of Raman experimental bands at 462, 768, 1180, 1599 and 2232 cm^{-1}. In the case of BN in silver sol, the present intensity enhancement calculation is in agreement with the one given in Ref. [15], in which frequencies belonging to class II (in-plane modes along *z*-axis) should be more enhanced if the benzene ring is adsorbed edge-on to the silver surface, that is, Raman bands observed at 461, 769, 1178, 1491 and 1599 cm^{-1}.

Table 9
Frontier orbital energies (a.u.) of the investigated systems

	Benzene	Benzene–Ag	BN	BN–Ag
LUMO	−0.009	−0.108	−0.063	−0.084
HOMO	−0.253	−0.260	−0.275	−0.280
Δ	0.252	0.152	0.212	0.196

LUMO benzene–Ag–FL = 0.094 a.u. (485 nm). FL–HOMO benzene–Ag = 0.058 a.u. (786 nm). LUMO BN–Ag–FL = 0.118 a.u. (386 nm). FL–HOMO BN–Ag = 0.078 a.u. (584 nm).

For the Ag coordination to benzene, very low frequencies are calculated at 23, 19 and 14 cm^{-1}, which are attributed to the long distance of the Ag atom (3.8 Å). Therefore, one can derive the more important EM mechanism acting in the SERS of this molecule. In case of BN frequencies assigned to vibrations with influence of the Ag atom were calculated at 81, 44 and 39 cm^{-1}, in agreement with a shorter calculated Ag–N distance (2.56 Å) in comparison with benzene–Ag distances. On the other hand, the most striking calculated enhanced bands intensities belong to the symmetric frequencies, so that a chemically enhanced mechanism can be considered for this molecule.

In order to determine the SERS mechanism, another aspect, the calculated energies of the frontier molecular orbital and the Ag Fermi level, are considered. For the Ag atom the experimental value of Fermi level (FL) has been reported to be −0.202 a.u. [48] This value is quite well reproduced at −0.207 a.u. in our calculations. The HOMO and LUMO energies for free benzene and BN as well as those for the molecule–Ag system are given in Table 9.

Energy gap values (ΔE) given in Table 9 reproduce quite well the λ_{max} of the benzene electronic spectrum (181 nm compared to 184 nm), while the λ_{max} for BN was calculated at 215 nm which is also very close to the one reported experimentally (about 220 nm) [49]. It is also observed in this table that the change in the HOMO–LUMO energy gap for benzene as a consequence of the metal influence is less drastic compared to the BN–Ag system, supporting the idea that for benzene the SERS mechanism should be mainly EM in nature.

For both systems, the Fermi level lies above the HOMO (Fig. 4), but well below the LUMO. Regarding a ligand to metal CT for BN, a HOMO–Fermi level difference of 0.078 a.u. (584 nm) is calculated for this molecule. This value is comparable to the laser excitation wavelength at 514 nm (0.089 a.u.) used in Ref. [15] to obtain the SERS spectrum of BN. That is, a suitable resonance is calculated in order to induce a ligand to metal CT process [42]. The higher metal–molecule CT energy in comparison with the excitation laser

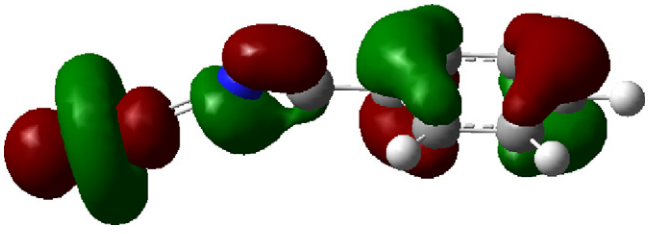

Fig. 4. HOMO of the BN–Ag system: the nitrogen lone pair and the occupied π system of BN interacting with a d_{z^2} orbital of the silver atom.

line allows us to interpret the BN SERS effect as chemisorption. A metal to ligand CT process can be ruled out as the required energy cannot come from the laser excitation.

4. Summary and conclusions

The model and the level of calculation used herein to study the Raman and SERS spectra of benzene and BN give reliable information on the geometrical parameters, internal force constants as well as frequencies and intensities of the distinct normal modes in order to gain insight in the orientation of benzene and BN on a Ag surface with respect to proper band assignments and SERS selection rules.

Theoretical concepts on SERS developed in literature are also well reproduced at our level of theory. Thus, the calculated energy gap HOMO–LUMO energy for benzene and BN reproduce quite well the electronic spectra of these molecules, while for the molecule–Ag systems the HOMO–LUMO energies allow us to distinguish between different SERS mechanisms, and to infer a main contribution of EM mechanisms in benzene and a ligand to metal CT in BN, in consonance with calculated Ag–molecule distances and the symmetric characteristics of the enhanced normal modes.

Acknowledgments

The authors acknowledge projects Fondecyt 1040640 and 107078. GDF also acknowledges DGI Universidad de Playa Ancha. RK is grateful for a generous allocation of computing time at the CSC, Uni Oldenburg.

References

[1] B.A. Hess Jr., J. Schaad, P. Carsky, R. Zahradnik, Chem. Rev. 86 (1986) 709.
[2] (a) M. Fleischman, P.J. Hendra, A.J. Maquillan, Chem. Phys. Lett. 26 (1974) 123;
(b) M.G. Albrecht, J.A. Creighton, J. Am. Chem. Soc. 99 (1977) 5215;
(c) A. Otto, in: M. Cardona, G. Guntherodt (Eds.), Light Scattering in Solids IV, Springer, Berlin, 1984, p. 289.
[3] W. Kohn, Rev. Mod. Phys. 71 (1998) 1253.
[4] H.P. Hohenberg, W. Kohn, Phys. Rev. B 136 (1964) 864.
[5] J.M. Seminario, P. Politzer (Eds.), Modern Density Functional Theory: A Tool for Chemistry, Elsevier, Amsterdam, 1995.
[6] C. Möller, M.S. Plesset, Phys. Rev. 46 (1934) 618.
[7] C.E. Blom, C. Altona, Mol. Phys. 31 (1976) 1377.
[8] T. Konishi, M. Fujitsuka, O. Ito, Y. Toba, Y. Usui, Bull. Chem. Soc. Jpn. 74 (2001) 1.
[9] J. Raap, S. Nieuwenhuis, A. Creemer, S. Hexspoor, U. Kragl, J. Lugtenburg, Eur. J. Org. Chem. 10 (1999) 2609.
[10] D. Dini, F. Decker, F. Andreani, E. Salatelli, P. Hapiot, Polymer 41 (2000) 6473.
[11] E. Lippert, W. Luder, E. Moll, W. Nagele, H. Boos, H. Prigge, I. Seilbold-Blankenstein, Angew Chem. 21 (1961) 695.
[12] A.M. Pathak, B.K. Sinha, Ind. J. Pure Appl. Phys. 19 (1981) 678.
[13] A.M. Pathak, B.K. Sinha, Ind. J. Pure Appl. Phys. 18 (1980) 619.
[14] B.H. Loo, Y.G. Lee, D.O. Frazier, Chem. Phys. Lett. 119 (1985) 312.
[15] D.W. Boo, K. Kim, M.S. Kim, Bull. Korean Chem. Soc. 8 (1987) 251.
[16] D.W. Boo, M.S. Kim, K. Kim, Bull. Korean Chem. Soc. 9 (1988) 311.
[17] X. Gao, J.P. Davies, M.J. Weaver, J. Phys. Chem. 94 (1990) 6858.
[18] M.F. Mrozek, S.A. Wasileski, M.J. Weaver, J. Am. Chem. Soc. 123 (2001) 12817.
[19] M.A. Palafox, V.K. Rastogi, L. Mittal, Int. J. Quantum Chem. 94 (2003) 189.
[20] A. Campion, P. Kambhampati, Chem. Soc. Rev. 27 (1998) 241.
[21] M.J. Frisch, G.W. Trucks, H.B. Schlegel, G.E. Scuseria, M.A. Robb, J.R. Cheeseman, J.A. Montgomery, Jr., T. Vreven, K.N. Kudin, J.C. Burant, J.M. Millam, S.S. Iyengar, J. Tomasi, V. Barone, B. Mennucci, M. Cossi, G. Scalmani, N. Rega, G.A. Petersson, H. Nakatsuji, M. Hada, M. Ehara, K. Toyota, R. Fukuda, J. Hasegawa, M. Ishida, T. Nakajima, Y. Honda, O. Kitao, H. Nakai, M. Klene, X. Li, J.E. Knox, H.P. Hratchian, J.B. Cross, C. Adamo, J. Jaramillo, R. Gomperts, R.E. Stratmann, O. Yazyev, A.J. Austin, R. Cammi, C. Pomelli, J.W. Ochterski, P.Y. Ayala, K. Morokuma, G.A. Voth, P. Salvador, J.J. Dannenberg, V.G. Zakrzewski, S. Dapprich, A.D. Daniels, M.C. Strain, O. Farkas, D.K. Malick, A.D. Rabuck, K. Raghavachari, J.B. Foresman, J.V. Ortiz, Q. Cui, A.G. Baboul, S. Clifford, J. Cioslowski, B.B. Stefanov, G. Liu, A. Liashenko, P. Piskorz, I. Komaromi, R.L. Martin, D.J. Fox, T. Keith, M.A. Al-Laham, C.Y. Peng, A. Nanayakkara, M. Challacombe, P.M.W. Gill, B. Johnson, W. Chen, M.W. Wong, C. Gonzalez, J.A. Pople, Gaussian 03, Revision B.05, Gaussian Inc., Pittsburgh, PA, 2003.
[22] A.D. Becke, J. Chem. Phys. 98 (1993) 1372.
[23] C. Lee, W. Yang, R.G. Parr, Phys. Rev. B 37 (1988) 785.
[24] T.H. Dunning, P.J. Hay, in: H.F. Schaefer (Ed.), Methods of Electronic Structure Theory, vol.2, Plenum Press, New York, 1977.
[25] P.J. Hay, W.R. Wadt, J. Chem. Phys. 82 (1985) 299.
[26] A.P. Scott, L. Radom, J. Phys. Chem. 100 (1996) 16502.
[27] W.B. Collier, QCPE Bull. 13 (1993) 19.
[28] R.F. Aroca, R.E. Clavijo, M.D. Halls, H.B. Schlegel, J. Phys. Chem. 104A (2000) 9500.
[29] T. Tanaka, A. Nakajima, A. Watanabe, T. Ohno, Y. Ozaki, Vib. Spectrosc. 34 (2004) 157.
[30] J. Casado, L. Nygaard, G.O. Sorensen, J. Mol. Struct. 8 (1971) 211.
[31] G. Portalone, A. Domenicvano, G.Y. Schultz, I. Hargittay, J. Mol. Struct. 160 (1987) 97.
[32] P. Diehl, J. Amrein, C.A. Veracini, Org. Magn. Reson. 20 (1988) 276.
[33] A.G. Csaszar, G. Fogarasi, Spectrochim. Acta 45A (1989) 845.
[34] C.W. Bock, M. Trachtman, P. George, J. Comput. Chem. 6 (1985) 592.
[35] N. Neto, M. Scrocco, S. Califano, Spectrochim. Acta A 22A (1966) 1981.
[36] C. La Lau, R.G. Snyder, Spectrochim. Acta 27A (1971) 2073.
[37] P. Pulay, G. Fogarasi, J.E. Boggs, J. Chem. Phys. 74 (1981) 3999.
[38] (a) G. Varsanyi, Assignments for Vibrational Spectra for 700 benzene Derivatives, Wiley, NY, 1974;
(b) J.H.S. Green, D.J. Harrison, Spectrochim. Acta 32A (1976) 1279.
[39] R.K. Chang, T. Furtak, Surface Enhanced Raman Scattering, Plenum, New York, 1982.
[40] B. Pettinger, in: J. Lipkowski, P.N. Ross (Eds.), Adsorption of Molecules at Metal Electrodes, VCH, New York, 1992, p. 285.
[41] J.R. Lombardi, R.L. Birke, T. Lu, J. Xu, J. Chem. Phys. 84 (1986) 4174.
[42] R.J.H. Clark, T.J. Dines, Angew. Chem. Int. Ed. Engl. 25 (1986) 131.
[43] A.M. Michael, J. Jiang, L. Brus, J. Phys. Chem. B 104 (2000) 11965.
[44] H. Grabhorn, A. Otto, Vacuum 41. (1990).
[45] A.C. Murray, Molecule–Silver separation dependence, in Ref. [39].
[46] J.A. Creighton, in: R.J.H. Clark, R.E. Hester (Eds.), Spectroscopy of Surfaces—Advances in Spectroscopy, vol. 16, Wiley, New York, 1988, p. 37, Chapter 2.
[47] Calculations with a linearly coordinated silver atom predicts a CN mode of benzonitrile at 2207 cm^{-1}, other geometries give values between 2173 and 2200 cm^{-1}. The frequency reported herein belongs to the most stable geometry, although differences are usually very small.
[48] N.W. Aschcroft, MerminF D.N., in Solid State Physics, W.B. Saunders Co., Philadelphia, London, Toronto, 1976.
[49] Y. Tsuzuki, Y. Asabe, J. Chem. Eng. Data 16 (1971) 108.